FLUKA CALCULATIONS OF NEUTRON SPECTRA AT BESSY *

K. Ott †, BESSY, Albert - Einstein - Str. 15, 12489 Berlin, Germany

Abstract

The synchrotron light source BESSY consists of a 50 MeV microtron, a full energy synchrotron and a 1.9 GeV storage ring. The electron losses during injection causes electromagnetic cascades within the stainless steel of the vacuum system and the aluminum vacuum chambers of the undulators. The cascade-produced neutrons results from giant resonances, quasi-deuteron fissions and photo-pion productions. The cross sections of the evaporation reactions of neutrons is an order of magnitude higher than the cross sections of the latter two reaction channels. The energy distribution of the giant resonance neutrons has a maximum at about 1 MeV in comparison with 100 - 200 MeV of the high energy neutrons. At electron accelerators outside the shielding wall half of the neutron dose is often determined by the more penetrating high energy part of the neutron fluence.

We used the particle interaction and transport code FLUKA for the calculations of both the fluence and the dose distribution inside and outside the shielding wall for different realistic scenarios.

From the integrated spectra we get the calibration factor for our neutron monitors, to determine the total neutron dose from the measurements directly.

INTRODUCTION

The storage ring BESSY II is in operation since 1998 and since 1999 used for a regular scientific program with synchrotron radiation. It has an extended double bend achromat lattice with a 16-fold symmetry. Up to 14 straight sections are suited for the installation for wigglers, undulators and wave length shifters (WLS). Two sections are used for the rf system and the injection septum. The full energy booster (1.9 GeV) operates in 10 Hz and is used asynchronously to fill the storage ring with bunch trains of 300 nsec. The short injection periods ($<$ 2 min and 3 to 5 times a day) are crucial for the annual radiation dose outside the shielding wall.

The electron losses at the vacuum system causes γ - radiation, giant - resonance neutrons quasi - deuteron fission neutrons and neutrons from photo - pion production.

In every ratchet at the closest transversal distance to the machine a stationary γ und neutron measurement system is installed outside the shielding wall in the experimental hall. The detectors are a ionisation chamber and a BF_3 counter and are sufficient to measure the pulsed γ and neutron radiation during injection without loss of information.

We discuss in this paper the contribution of the high energy neutrons that cannot be detected by our neutron monitors. This is the first time that such an investigation is conducted at a synchrotron light source.

NEUTRON DOSES

In two papers Tesch [1] described the neutron doses at electron accelerators as sum of giant resonance neutrons and fast neutrons for thick iron or copper targets:

$$Hr^2 = 9.55 \cdot 10^{-16} \cdot Ee^{\frac{-d\cdot\rho}{\lambda_{gr}}} + 4.0 \cdot 10^{-17} \cdot Ee^{\frac{-d\cdot\rho}{\lambda_{he}}} \quad (1)$$

H in Sv/$e-$, r in m, E in GeV, d in cm, λs in $\mathrm{g/cm^2}$. Recommended values are for normal concrete λ_{gr} = 37 $\mathrm{g/cm^2}$; λ_{he} = 100 $\mathrm{g/cm^2}$. In case of an aluminum target the first term has to be multiplied by 0.43 and the second term by 1.6 and λ_{gr} = 47.6 $\mathrm{g/cm^2}$. The high energy term can be applied for lateral shielding only. For thin targets Tesch gives for the high energy term a correction factor, that is 0.1 if the length of the target is about 1 radiation length.

For thick copper targets and lateral shielding the results of the two neutron contributions are according to Hoefert et al [2]

$$Hr^2 = 1.11 \cdot 10^{-15} \cdot Ee^{\frac{-d\cdot\rho}{\lambda_{gr}}} + 1.4 \cdot 10^{-17} \cdot Ee^{\frac{-d\cdot\rho}{\lambda_{he}}} \quad (2)$$

Recommended values are for normal concrete λ_{gr} = 42 $\mathrm{g/cm^2}$; λ_{he} = 117 $\mathrm{g/cm^2}$. For iron target the first factor changes to $7.8 \cdot 10^{-15}$, the second to $1.5 \cdot 10^{-17}$. In case of an aluminum target the two factors are $6.1 \cdot 10^{-15}$ and $2.0 \cdot 10^{-17}$. For thin targets there is a correction factor for the giant resonance term, that is also 0.1 if the target length is 1 radiation length. For the high energy term no correction factor for thin targets is given.

A more recent approach is given by Dinter et al [3] that is based on FLUKA calculations. For thick targets and concrete shielding they found:

$$\begin{aligned} Hr^2 &= a_1 \cdot Ee^{\frac{-d\cdot\rho}{\lambda_{gr}}} + a_2 \cdot E^{1.1} e^{\frac{-d\cdot\rho}{\lambda_{he}}} \quad (3)\\ a_1 &= 2.4 \cdot 10^{-17} \cdot A^{2/3}(0.33 + 0.67\sin\theta)\\ a_2 &= 2.3 \cdot 10^{-15} \cdot A^{-2/3}(0.07 + 0.93e^{-\theta/31^0})\\ \lambda_{he} &= 91 + 53 \cdot e^{-\theta/33^0} \end{aligned}$$

θ is the angle of observation, $\lambda_{gr} = 28\mathrm{g/cm^2}$, A is the atomic mass number of the target. The other symbols and units are the same as for the other formulas. No correction for thin targets is given and the only considered shielding material is normal concrete.

* funded by the Bundesministerium für Bildung, Wissenschaft, Forschung und Technologie and by the Land Berlin

† Email: ott@bessy.de

FLUKA CALCULATIONS

We calculate the neutron spectra as pSv/(primary electron) as ambient dose equivalent $H^*(10)$ from the fluences at run time. FLUKA [4] uses the fluence to dose conversion coefficients [5] for a antero-posterior geometry or other geometries if these results in higher doses, which is the case at neutron energies > 50 MeV.

We use a logarithmic binning up to the neutron energy of 500 MeV for transversal and 1 GeV for longitudinal directions and down to thermal energies. In our spectra figures the group doses are divided by the lethargy interval $\ln E_{i+1} - \ln E_i$ (i is the respective bin number). We use boundary crossing estimators with different detector areas.

At the ratchets we have three openings for beam lines at 0^0 from insertion devices, 4^0 and 6.7^0 from the first dipol. The shielding wall in forward direction at the beamline angles consist of a 5 cm lead screen and 1 m heavy concrete, in the transversal direction the shielding wall consists of 1 m normal concrete.

In our tables H_{10-}, H_{10+} means the integrated doses from the spectra for energies < 10 MeV and > 10 MeV respectivly. H_Σ is the dose that results from the full integral of the spectrum, $H_\Sigma^{(i)}$ is the dose that results from the semi-empirical formula i respectivly. Every H value is given as pSv/primary electron.

Thick copper targets (spherical geometry) To compare our results with the results of Dinter et al. [3] we start with a thick copper target that is located in the center of a hollow concrete sphere. The radius of the hollow space is 5 m. The thick copper target (l=22 cm,r=4 cm), surrounded by vacuum, is hit by a pencil like electron beam. As detector area we use a spherical ring around the beam axis, that corresponds to an angle range between 80 and 100 degrees. At 30 GeV electron energy our results agree well with [3], so we repeated the calculations with the BESSY energy of 1.9 GeV. The length of the copper target we kept, because we considered only the transversal direction with this geometry. The result is shown in fig. 1.

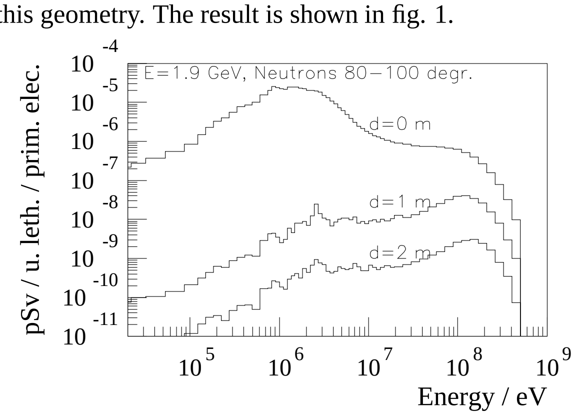

Figure 1: Neutron spectra thick from Cu target at 90^0

At the depth of 2 m concrete the contribution of the former giant resonance neutrons are neglectable. On the other hand two thirds of the former high energy neutrons are

Table 1: Results for thick Cu targets at 90^0, r=5 m $+d$

d/m	H_{10-}	H_{10+}	H_{10+}/H_{10-}	
0	5.44E-05	2.34E-06	0.043	
1	2.52E-08	7.01E-08	2.787	
2	1.38E-09	5.05E-09	3.653	
d/m	H_Σ	$H_\Sigma^{(1)}$	$H_\Sigma^{(2)}$	$H_\Sigma^{(3)}$
0	5.68E-05	7.66E-05	8.47E-05	3.05E-05
1	9.53E-08	3.13E-07	3.48E-07	9.06E-08
2	6.43E-09	1.57E-08	1.17E-08	5.42E-09

slowed down to energies typical for giant resonance neutrons. Beyond the concrete thickness of 1 m the hardening effects on the spectrum are small because of the radiation equilibrium of high and low energy neutrons. As can be seen in table 1 the agreement is best with eq. 3.

Thick aluminum targets (BESSY geometry) The aluminum vacuum chambers of the undulators are the locations with the smallest mechanical aperture in the storage ring. They have a rectangular outline and the cross-sectional area of the aperture is elliptic. The height of the aperture is 11 mm, the material thickness in both vertical directions is 1 mm. To left side a slit to a second cave exists, where the getter pumps are connected. The material thickness to the side is 15 mm. We consider a scenario, where the electron beams hit the side of the vacuum chamber with an angle of 1 mrad. The distance to the side wall is 1 m. In fig.2 the dose rate at an injection under crash conditions (100% losses) is calculated. We use circular detector areas, whose radii correspond to an angular range between 80 and 100 degrees. The results are given in fig. 3 and table 2. The agreement is again best with eq. 3.

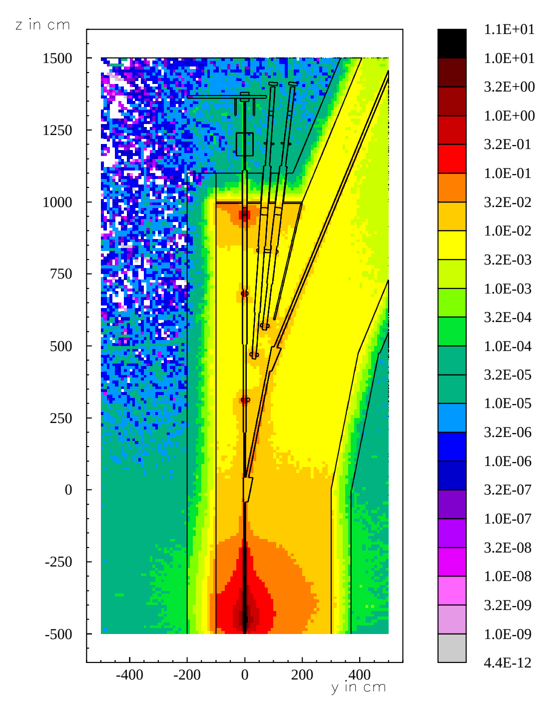

Figure 2: Al target BESSY geometry, I = 3.8E10 $e-$/s

Table 2: Results for thick Al targets at 90^0, r=1 m +d

d/m	H_{10-}	H_{10+}	H_{10+}/H_{10-}	
0	4.55E-04	5.61E-05	0.123	
1	2.85E-07	7.53E-07	2.637	
d/m	H_{Σ}	$H_{\Sigma}^{(1)}$	$H_{\Sigma}^{(2)}$	$H_{\Sigma}^{(3)}$
0	5.11E-04	1.09E-03	1.19E-03	4.73E-04
1	1.04E-06	4.98E-06	2.53E-06	1.40E-06

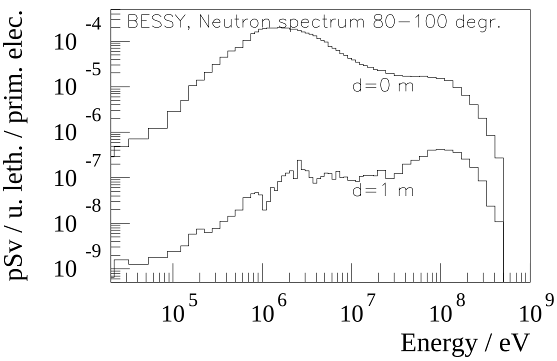

Figure 3: Neutron spectra at 90^0, Al-Target

Thin Fe targets (BESSY geometry) The dipoles are the locations where β_x is largest. If the electron beam hits the vacuum chamber (d = 2 mm) of the first dipole at half of the deflection angle, the effective length in the iron is about one radiation length. We use here a 2.0 cm thick (radius 2.5 cm) target on which the pencil like electron beam of 1.9 GeV hits at normal incident. We use the same circular detector areas as in the second scenario. The results are shown in fig. 4 and table 3. The agreement can be improved if the correction for the thin targets is applied to both terms of the semi-empirical formulas, thereby decreasing their values by the factor 10.

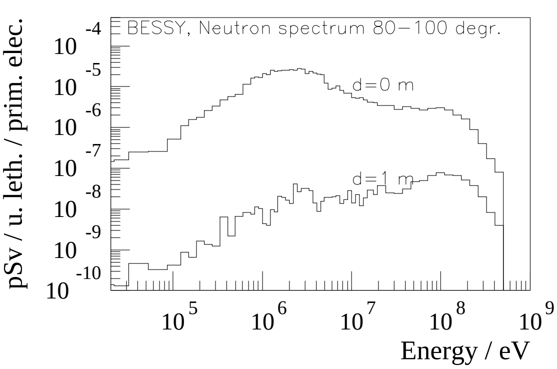

Figure 4: Neutron spectra at 90^0, thin Fe target

RESULTS

We found best agreements with our calculated doses and the semi-empirical formula of [3] for thick targets in transversal und thin targets in forward directions. For thin targets and transversal directions the high energy term of this formula should be corrected by the correction factors of [1] and the low energy term by the correction factor of [2] which gives for the iron target both the value of 0.1.

Table 3: Results for thin Fe target at 90^0, r=1 m +d

d/m	H_{10-}	H_{10+}	H_{10+}/H_{10-}	
0	5.94E-05	9.75E-06	0.164	
1	5.38E-08	1.43E-07	2.655	
d/m	H_{Σ}	$H_{\Sigma}^{(1)}$	$H_{\Sigma}^{(2)}$	$H_{\Sigma}^{(3)}$
0	6.91E-05	1.89E-03	1.49E-03	7.05E-04
1	1.97E-07	2.82E-06	2.53E-06	8.89E-07

At BESSY the highest dose rates are possible from transversal scenarios. The reason is the greater distance in the forward direction and the larger absorption coefficient for heavy concrete that is more effective against high energy neutrons. This overcompensates the higher doses of high energy neutrons in forward direction. From our three scenarios we found behind 1 m of normal concrete for thick copper, thin iron and thick aluminum targets for the relation H_{10+}/H_{10-} the values of 2.787, 2.655 and 2.637. Because there are no thick copper targets in the vacuum system of the storage ring we get 2.65 as H_{10+}/H_{10-} mean value. In the forward direction the relations H_{10+}/H_{10-} for the thin iron and the thick aluminum target are 1.420 and 0.689. The transversal neutron dose is an order of magnitude higher than the longitudinal one at BESSY outside the shielding walls, therefore we use the calibration factor derived from the transversal doses. Because H_{10+} cannot be deteced by our neutron monitors , the measured neutron values have to be multiplied by the factor 3.65 to get the real neutron doses at BESSY. But even then the 1 mSv/a limit is hold in the accessible part of the experimental hall at BESSY.

REFERENCES

[1] K. Tesch, Part. Acc. **9**, p201 (1979), Rad. Prot. Dosi. **22,1**, p27 (1988)

[2] Landolt - Börnstein, Numerical Data in Science and Technology, vol. 11, Springer, Berlin (1990)

[3] H. Dinter, A. Leuschner, K. Tesch, D. Dworak, L. Loskiewicz, NIM A **455**, p460 (2000)

[4] A. Fassò, A. Ferrari, J. Ranft, and P.R. Sala, ”FLUKA: a multi-particle transport code”, CERN Yellow Report (2005), INFN/TC05/11, SLAC-R-773, in press A. Fassò, A. Ferrari, S. Roesler, P.R. Sala, G. Battistoni, F. Cerutti, E. Gadioli, M.V. Garzelli, F. Ballarini, A. Ottolenghi, A. Empl and J. Ranft, ”The physics models of FLUKA: status and recent developments”, Computing in High Energy and Nuclear Physics 2003 Conference (CHEP2003), La Jolla, CA, USA, March 24-28, 2003, (paper MOMT005), eConf C0303241 (2003), arXiv:hep-ph/0306267

[5] ICRP Publication 74, Pergamon Press (1996); A. Ferrari, M. Pelliccioni Rad. Prot. Dosi. **77**. p159 (1998)